

Basic Study

Dextran sulfate sodium-induced acute colitis impairs dermal lymphatic function in mice

Germaine D Agollah, Grace Wu, Ho-Lan Peng, Sunkuk Kwon

Germaine D Agollah, Grace Wu, Sunkuk Kwon, Center for Molecular Imaging, The Brown Foundation Institute of Molecular Medicine, The University of Texas Health Science Center, Houston, TX 77030, United States

Germaine D Agollah, The University of Texas Graduate School of Biomedical Sciences at Houston, The University of Texas MD Anderson Cancer Center, Houston, TX 77030, United States

Ho-Lan Peng, The University of Texas Health Science Center at Houston, School of Public Health, Houston, TX 77030, United States

Author contributions: Agollah GD, Wu G and Kwon S contributed to the acquisition and interpretation and statistical analysis of *in vivo* and *ex vivo* data; Peng HL performed statistical analysis; Kwon S designed and supervised the research; Agollah GD and Kwon S wrote the manuscript.

Supported by (in part) A pilot/feasibility grant from NIH/ National Institute of Diabetes and Digestive and Kidney Disease, Center Grant P30 DK56338 (for Kwon S); the Schissler Foundation Fellowship for Translational Studies of Common Human Diseases (for Agollah GD).

Institutional review board statement: The study was reviewed and approved by University of Texas Health Science Center Institutional Review Board.

Institutional animal care and use committee statement: All animal experiments were reviewed and approved by University of Texas Health Science Center Institutional Animal Welfare Committee (AWC-14-0034).

Conflict-of-interest statement: The authors declared that they have no conflicts of interest to this work.

Data sharing statement: No additional data are available.

Open-Access: This article is an open-access article which was selected by an in-house editor and fully peer-reviewed by external reviewers. It is distributed in accordance with the Creative Commons Attribution Non Commercial (CC BY-NC 4.0) license, which permits others to distribute, remix, adapt, build upon this

work non-commercially, and license their derivative works on different terms, provided the original work is properly cited and the use is non-commercial. See: <http://creativecommons.org/licenses/by-nc/4.0/>

Correspondence to: Sunkuk Kwon, PhD, Assistant Professor, Center for Molecular Imaging, The Brown Foundation Institute of Molecular Medicine, The University of Texas Health Science Center, 1825 Pressler Street, SRB 330F, Houston, TX 77030, United States. sunkuk.kwon@uth.tmc.edu
Telephone: +1-713-5003563
Fax: +1-713-5000319

Received: May 16, 2015
Peer-review started: May 20, 2015
First decision: June 19, 2015
Revised: July 10, 2015
Accepted: August 31, 2015
Article in press: August 31, 2015
Published online: December 7, 2015

Abstract

AIM: To investigate whether dermal lymphatic function and architecture are systemically altered in dextran sulfate sodium (DSS)-induced acute colitis.

METHODS: Balb/c mice were administered 4% DSS in lieu of drinking water *ad libitum* for 7 d and monitored to assess disease activity including body weight, diarrhea severity, and fecal bleeding. Control mice received standard drinking water with no DSS. Changes in mesenteric lymphatics were assessed following oral administration of a fluorescently-labelled fatty acid analogue, while dermal lymphatic function and architecture was longitudinally characterized using dynamic near-infrared fluorescence (NIRF) imaging following intradermal injection of indocyanine green (ICG) at the base of the tail or to the dorsal aspect of the left paw prior to, 4, and 7 d after DSS

administration. We also measured dye clearance rate after injection of Alexa680-bovine serum albumin (BSA). NIRF imaging data was analyzed to reveal lymphatic contractile activity after selecting fixed regions of interest (ROIs) of the same size in fluorescent lymphatic vessels on fluorescence images. The averaged fluorescence intensity within the ROI of each fluorescence image was plotted as a function of imaging time and the lymphatic contraction frequency was computed by assessing the number of fluorescent pulses arriving at a ROI.

RESULTS: Mice treated with DSS developed acute inflammation with clinical symptoms of loss of body weight, loose feces/watery diarrhea, and fecal blood, all of which were aggravated as disease progressed to 7 d. Histological examination of colons of DSS-treated mice confirmed acute inflammation, characterized by segmental to complete loss of colonic mucosa with an associated chronic inflammatory cell infiltrate that extended into the deeper layers of the wall of the colon, compared to control mice. *In situ* intravital imaging revealed that mice with acute colitis showed significantly fewer fluorescent mesenteric lymphatic vessels, indicating impaired uptake of a lipid tracer within mesenteric lymphatics. Our *in vivo* NIRF imaging data demonstrated dilated dermal lymphatic vessels, which were confirmed by immunohistochemical staining of lymphatic vessels, and significantly reduced lymphatic contractile function in the skin of mice with DSS-induced acute colitis. Quantification of the fluorescent intensity remaining in the depot as a function of time showed that there was significantly higher Alexa680-BSA fluorescence in mice with DSS-induced acute colitis compared to pre-treatment with DSS, indicative of impaired lymphatic drainage.

CONCLUSION: The lymphatics are locally and systemically altered in acute colitis, and functional NIRF imaging is useful for noninvasively monitoring systemic lymphatic changes during inflammation.

Key words: Dextran sulfate sodium; Colitis; Lymphatic system; Inflammation; Near-infrared fluorescence imaging

© **The Author(s) 2015.** Published by Baishideng Publishing Group Inc. All rights reserved.

Core tip: Inflammatory bowel disease (IBD) is a systemic disease, as it is often associated with extra-intestinal manifestations, complications, and other autoimmune disorders. However, it is unknown whether dermal lymphatic function changes systemically in response to IBD. In this study, we employed near-infrared fluorescence imaging to characterize dermal lymphatic function and architecture in mice with dextran sulfate sodium (DSS)-induced acute colitis. Our results demonstrated impaired lymphatic function in mesenteric lymphatics accompanied by dilated lymphatic vessels and reduced lymphatic contractility

in the skin of mice with DSS-induced acute colitis, indicating that DSS-induced acute colitis results in systemic lymphatic dysfunction.

Agollah GD, Wu G, Peng HL, Kwon S. Dextran sulfate sodium-induced acute colitis impairs dermal lymphatic function in mice. *World J Gastroenterol* 2015; 21(45): 12767-12777 Available from: URL: <http://www.wjgnet.com/1007-9327/full/v21/i45/12767.htm> DOI: <http://dx.doi.org/10.3748/wjg.v21.i45.12767>

INTRODUCTION

Inflammatory bowel disease (IBD), such as ulcerative colitis (UC) and Crohn's disease (CD), involves progressive and destructive inflammation of the small and large intestines. Recent evidence suggests that IBD pathogenesis may result from an abnormal immune response to normal gut microbial antigens within the intestinal flora of genetically-susceptible individuals^[1]. However, the precise mechanisms of immune and genetic involvement in IBD remain poorly understood.

IBD is a systemic disease, as it is often associated with extra-intestinal manifestations (EIMs), complications, and other autoimmune disorders including psoriasis and rheumatoid arthritis^[2]. Cutaneous complications, such as erythema nodosum and pyoderma gangrenosum, are relatively common manifestations of IBD^[3,4]. Although dependent on different mechanisms, both IBD and its extra-intestinal complications are characterized by an influx of destructive inflammatory cells with the subsequent secretion of pro-inflammatory cytokines and mediators, which may affect lymphatic function, both locally and systemically. A previous study demonstrated increased lymphatic vessel diameters, reduced number of spontaneously-pumping lymphatic vessels, and lower contraction frequency *in vitro* and *in situ* in the mesenteric lymphatic vessels in the 2,4,6-trinitrobenzene sulfonic acid (TNBS) model of guinea pig ileitis^[5]. Impaired lymphatic function during intestinal inflammation may delay immunological responses and thus hinder the resolution of inflammation-associated edema^[6], a common condition associated with IBD^[7,8]. However, it is unknown whether the lymphatic system changes systemically in response to gut inflammation.

The lymphatic system plays important roles in: (1) removing excess fluid from the tissues and thus maintaining tissue-fluid homeostasis; and (2) transporting activated immune cells into draining lymph nodes (DLNs) *via* afferent lymphatic vessels, thus evoking inflammatory immune response and subsequently resolving inflammation^[9,10]. Impaired lymphatic function has been implicated in many pathological conditions, including inflammation^[10]. Given the essential role played by the lymphatics in the initiation, progression, and resolution of inflammation,

lymphatic function may be systemically altered during gut inflammation. Additionally, intestinal lymphatic vessels, known as lacteals, within intestinal villi take up dietary lipids for transportation back to the blood vasculature. Thus, it is likely that lymphatics play an important role in the complex etiology of IBD and its EIMs^[6]. Herein, we describe lymphatic function in the skin of mice with DSS-induced acute colitis using near-infrared fluorescence (NIRF) lymphatic imaging^[11]. Our data demonstrates for the first time, systemically-altered dermal lymphatic function in mice with acute colitis.

MATERIALS AND METHODS

Animals

Six to eight week-old female Balb/c mice (Charles River) were housed and fed sterilized pelleted food and sterilized drinking water. Animals were maintained in a pathogen-free mouse facility accredited by the American Association for Laboratory Animal Care (AALAC). All experiments were performed in accordance with the guidelines of the Institutional Animal Care and Use Committee (IACUC). Animal experiments were approved by University of Texas Health Science Center Institutional Animal Welfare Committee (AWC-14-0034).

Induction of colitis and assessment of disease severity

Experimental colitis was induced by administering 4% (wt/vol) DSS (molecular weight 36-50 kDa, MP Biomedicals)^[12] solution to replace drinking water *ad libitum* for 7 d. Control mice received standard drinking water. On day 7, mice were euthanized and tissues harvested for *ex vivo* studies. In all mice, body weight and diarrhea severity (diarrhea score: 0, normal; 1, slightly loose feces; 2, loose feces; 3, watery diarrhea) were monitored^[13]. Body weight at day 4 and 7 were normalized to day 0, and body weight change expressed as a percentage. In addition, fecal bleeding (visible fecal blood score: 0, normal; 1, slightly bloody; 2, bloody; 3, blood in whole feces) was scored^[13]. Colon length was measured to determine severity of colitis.

In situ Mesenteric lymphangiography imaging

For imaging mesenteric lymphatic vessels, 1 mL of a long-chain fatty acid, Bodipy-FL-C16 (Life Technologies) was orally administered to control mice and 7-d DSS-treated mice. At 30 min after oral administration, mice were euthanized and fluorescence imaging was performed to visualize fluorescent lymphatic vessels in the mesentery using a stereomicroscope (MZ16 A, Leica Microsystems, Inc.) with excitation light at 493 nm and emission light at 503 nm. The number of fluorescent mesenteric lymphatic vessels was counted.

In vivo functional NIRF lymphatic imaging

Mice were imaged for baseline lymphatic parameters prior to beginning DSS treatment, at 4, and 7 d

after administration. Mice were anesthetized with isoflurane and maintained at 37 °C on a warming pad. A volume of either 10 µL or 2 µL of 645 µmol/L ICG (Akorn, Inc.) dissolved in mixture of distilled water and 0.9% sodium chloride in a volume ratio of 1:9 was injected intradermally at either the base of the tail or to the dorsal aspect of left hind paw, respectively, using 31 gauge needles (BD Ultra-Fine™ II Short Needle, Becton and Dickinson Medical) or 34 gauge needles (Nanofil, World Precision Instruments, Inc.). Fluorescence images were acquired immediately before and for up to 20 min after id injection using a custom-built NIRF imaging system as described previously^[14]. The number of fluorescent lymphatics in the dorsum of the foot or the base of the tail near the injection site was counted.

Quantification of dye clearance

In order to measure dye clearance, 2 µL of Alexa680-BSA was injected intradermally at the dorsal aspect of the left hind paw in an anesthetized mouse prior to DSS treatment for baseline, and 7 d after DSS treatment using 34 gauge needles (Nanofil, World Precision Instruments, Inc.). The injection area in a mouse was imaged every 1 h for up to 6.5 h after injection. Mice regained consciousness between measurements. The region of interest (ROI) was defined as the entire paw and fluorescent intensities within the ROI were measured.

Immunohistochemical analysis

For histological analysis, tissue samples were fixed in 10% formalin overnight before transfer into 70% ethanol. Tissue samples were embedded in paraffin and 4 µm sections used in all staining procedures. The tissue sections stained with hematoxylin-eosin (HE) were analyzed by Dr. Roger Price at Center for Comparative Medicine Pathology Core at Baylor College of Medicine (BCM). Paraffin-embedded sections were stained for LYVE-1 as follows. Following paraffin removal and antigen retrieval using citrate buffer, tissues were blocked with 5% bovine serum albumin (BSA) and stained with rabbit anti-mouse LYVE-1 antibody (AngioBio) and biotin-anti rabbit secondary antibody (Vector Labs). Vectastain Elite ABC system for peroxidase and DAB or ImmPACT Novared chromagen reagents were used before tissues were counter-stained with hematoxylin (Vector Labs). LYVE-1 expression in three different fields in each section was examined at magnification × 400 (Leica Microsystems Inc.). Lymphatic vessel number and relative lymphatic vessel area, which was defined as the percentage of positively stained lymphatic vessel area were determined as described previously^[15] using Image-Pro Plus software (Media Cybernetics, Inc.).

Lymphatic function analysis

The data was analyzed with Matlab (The MathWorks,

Inc.) and ImageJ (National Institutes of Health). To reveal contractile activity resulting in propulsive lymph flow, fixed regions of interest (ROIs) of equal size in the fluorescent lymphatic vessels were defined on fluorescence images. The averaged fluorescence intensity within each ROI in each fluorescence image was plotted as a function of imaging time. The number of “pulses” of ICG-laden lymph was an indication of lymphatic contractile activity and termed as “contractions”.

Statistical analysis

Data were presented as average values \pm standard error. The statistical analysis was performed by Ho-Lan Peng from School of Public Health, The University of Texas Health Science Center at Houston, using SAS Enterprise Guide 5.1 and SigmaPlot 11.0. For the pairwise comparisons, the paired *t* test or Wilcoxon signed rank test were used depending on the type and the normality of the data. For between group comparisons, the two-sample *t* test or Wilcoxon rank sum test were used depending on the normality of the data. The significance level was defined as $P < 0.05$.

RESULTS

Characteristics of DSS-induced acute colitis

Mice treated for 7 d with DSS developed acute inflammation. As shown in Figure 1, clinical symptoms in mice with DSS-induced acute colitis included loss of body weight (Figure 1A), loose feces/watery diarrhea (Figure 1B), and fecal blood (Figure 1C), all of which were aggravated as disease progressed to 7 d. In addition, the length of the colon decreased as disease severity increased and was significantly shorter in mice at day 7 (Figure 1D). Histopathological examination of colons of DSS-treated mice confirmed acute inflammation (Figure 1F), characterized by segmental to complete loss of the colonic mucosa with an associated chronic inflammatory cell infiltrate that extended into the deeper layers of the wall of the colon, compared to control mice (Figure 1E). Ulceration of the colon was typically associated with hyperplasia of the colonic mucosa adjacent to the areas of ulceration. Thus, mice treated with DSS for 7 d exhibited acute inflammation as assessed by clinical symptoms.

DSS treatment induces mesenteric and dermal lymphatic vessel remodeling

To assess whether DSS-induced colitis affected mesenteric lymphatic drainage, we performed intravital fluorescent lymphangiography 30 min after oral gavage administration of Bodipy-FL-C16. Mice with acute colitis (Figure 2B) showed impaired uptake of Bodipy-FL-C16 within mesenteric lymphatics as compared to controls (Figure 2A). We observed significantly fewer fluorescent mesenteric lymphatic

vessels in mice treated with DSS for 7 d than those in control mice (Figure 2E). To examine differences in lymphatic vessel architecture within the colons, we performed immunohistochemical (IHC) staining for lymphatic vessel endothelial hyaluronan receptor 1 (LYVE-1). Colons of DSS-treated mice exhibited dilated lymphatic vessels (Figure 2D and G) and increased number of vessels (Figure 2F), compared to control mice (Figure 2C).

Given the changes within the mesenteric lymphatics, we next assessed whether DSS-induced colitis affected peripheral lymphatic architecture and function as well. We performed NIRF imaging after id injection of ICG in the dorsal aspect of the hind paw. *In vivo* fluorescence imaging data demonstrated that mice with acute colitis after 7 d of DSS treatment (Figure 3B) showed similar peripheral lymphatic drainage patterns in the paw as compared to control animals (Figure 3A), although dilated lymphatic vessels were observed in mice with DSS-induced colitis. However, the number of fluorescent lymphatic vessels in the foot between baseline (2.2 ± 0.4) and 7 d after DSS treatment (1.8 ± 0.4) was not statistically different. We also assessed the depot clearance of Alexa680-BSA. Fluorescent images from one representative mouse showing clearance of Alexa680-BSA from the depot (dorsal aspect of the left hind paw) over about 6 h are shown in Figure 3C. We found that while the fluorescence rapidly decreased in mice prior to DSS treatment, 7 d DSS treatment delayed the clearance. Quantification of the fluorescent intensity remaining in the depot as a function of time as shown in Figure 3D, showed that there was significantly higher fluorescence in mice with DSS-induced acute colitis than that in mice prior to DSS treatment, indicative of impaired lymphatic drainage.

Next, to examine whether dermal lymphatics were altered in response to DSS-treatment, skin and ear tissues were immunostained with antibody to LYVE-1. We observed no significant differences in the number of lymphatic vessels between control (Figure 4A and E) and mice with DSS-induced colitis (Figure 4B and F) in either skin or ears, whereas a significant increase of the relative area occupied by peripheral lymphatic vessels in mice with DSS-induced colitis was observed as compared to that in control, indicative of dilated dermal lymphatic vessels in response to DSS-induced acute colitis (Figure 4C, D, G and H). However, we did not observe any clinically apparent manifestations in the skin of DSS-treated mice.

DSS-induced colitis impairs dermal lymphatic contractile function

We examined lymphatic contractile function in the skin of mice with DSS-induced acute colitis to investigate whether lymphatic function was systemically impaired in response to intestinal inflammation. Quantitative analysis of lymphatic contractile function demonstrated

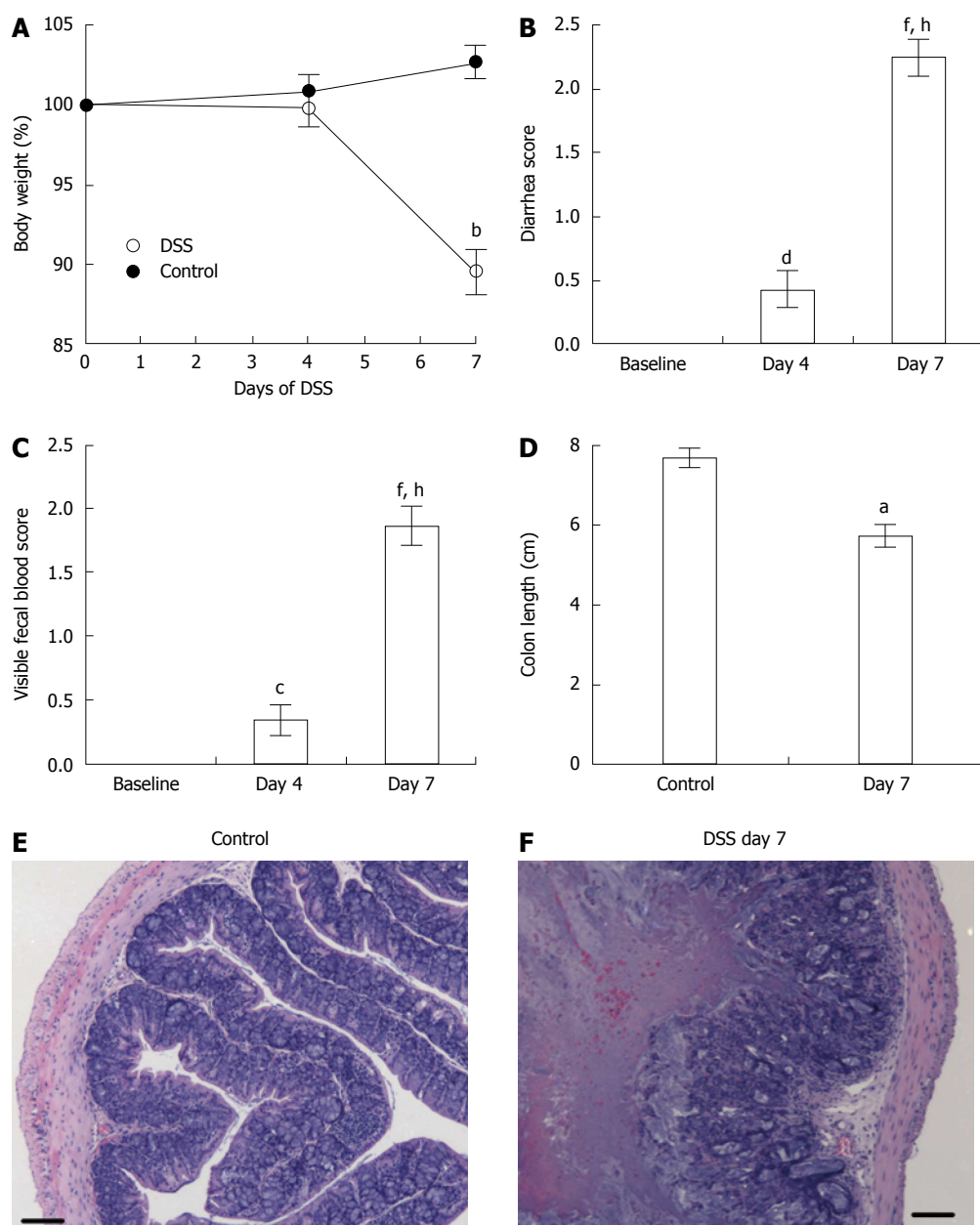


Figure 1 Clinical and inflammatory symptoms during dextran sulfate sodium-induced acute colitis assessed by changes in body weight (A), diarrhea score (B), visible fecal blood score (C), colon length (D), and histological sections of the colons in control mice (E) and mice that received dextran sulfate sodium for 7 d (F). Control ($n = 9$) and dextran sulfate sodium (DSS)-treated ($n = 21$) mice. Data presented as mean \pm SE. ^a $P < 0.05$, ^b $P < 0.001$ vs control. ^c $P < 0.05$, ^d $P < 0.01$, ^e $P < 0.001$ vs baseline. ^f $P < 0.001$ vs day 4. Scale bar = 100 μ m.

significant reduction of lymphatic contraction frequency at day 4 in the popliteal afferent pre-nodal lymphatic vessels (Figure 5B) in DSS-treated mice, which further decreased at day 7, which correlated to increased disease severity (Figure 1). In addition, there were significantly decreased lymphatic contraction frequencies at day 4 and 7 in the popliteal post-nodal efferent lymphatic vessel of DSS-treated mice as compared to the baseline data (Figure 5C). On the other hand, both afferent and efferent lymphatic contractility in control mice remained unchanged from baseline to day 7.

DISCUSSION

The purpose of this study was to characterize changes in lymphatic function and architecture in a chemically-induced murine model of colitis. We utilized *in situ* lymphangiography and non-invasive NIRF imaging techniques to investigate dermal lymphatic response during gut inflammation. As DSS-induced colitis progressed (Figure 1), we observed alterations in mesenteric lymphatics (Figure 2), peripheral lymphatic flow (Figure 3), and dermal lymphatic architecture (Figure 4). Additionally, there was a gradual reduction

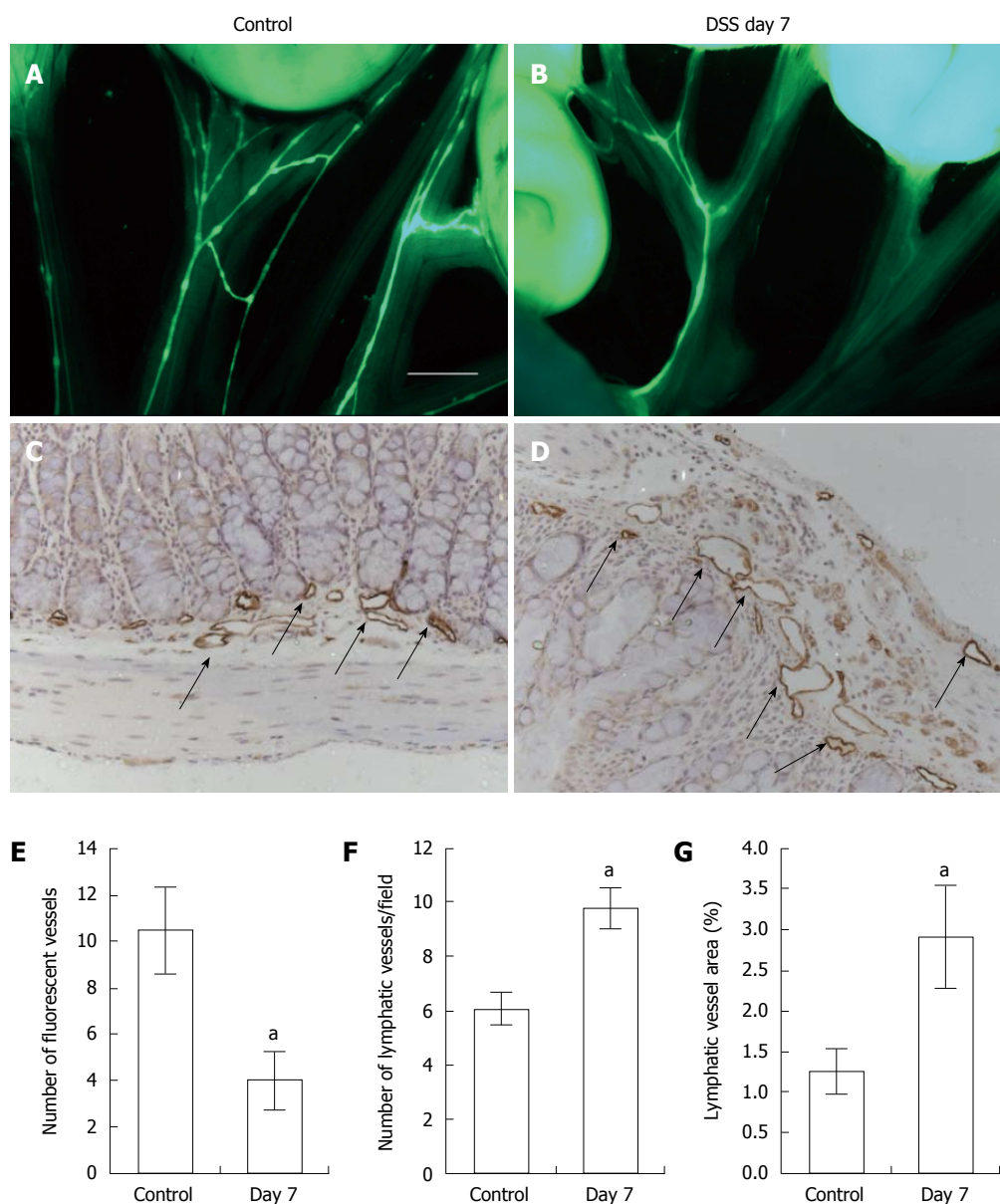


Figure 2 Intravital fluorescent lymphangiography 30 min after oral gavage administration of Bodipy-FL-C16. Lymphangiography showing mesenteric lymphatic drainage in control (A, $n = 4$) and mice with dextran sulfate sodium (DSS)-induced colitis (B, $n = 5$) after oral gavage of 1 mL of Bodipy-FL-C16. Significantly reduced number of fluorescent mesenteric lymphatic vessels was observed in mice with DSS-induced colitis as compared to control mice (E). Scale bar = 2 mm. IHC assessment of lymphatic vessels using antibody against LYVE-1 in the colon of control (C) and mice with DSS-induced colitis (D) and quantification of number of lymphatic vessels (F) and vessel area (G) in colons. Data presented as mean \pm SE. ^a $P < 0.05$ control vs DSS day 7.

in lymphatic contractility in the skin of DSS-treated mice (Figure 5), suggesting that DSS-induced acute colitis has a significant impact on both local and systemic lymphatic function.

IBD, including UC and CD, is an autoimmune disorder of unknown etiology that mainly involves the intestines^[16]. Previous studies showed functional and structural changes in the blood vasculature, such as dilated and tortuous vessels with increased vascularity and changes in intestinal blood flow, in patients with IBD and chemically-induced murine models of colitis^[17,18]. In addition to vascular alterations, submucosal edema, possibly due to impaired lymphatic function, has previously been observed in intestinal lymphatics in

IBD^[6-8]. Increased lymphangiogenesis has also been observed in patients with and experimental models of IBD^[6,19] as observed in our study (Figure 1). Previous data demonstrated that mice lacking angiopoietin-2, which exhibit disorganized and hyperplastic lymphatic vasculature, have exaggerated disease activity in the DSS colitis model, indicating that the lymphatic system plays an important role in IBD^[20]. Recent studies have also demonstrated that vascular endothelial growth factor receptor (VEGFR)-3 blockade caused inhibition of disease resolution in animal models of colitis and adenoviral induction of VEGF-C provided increased protection against the development of DSS-induced acute and chronic colitis as a result of increased

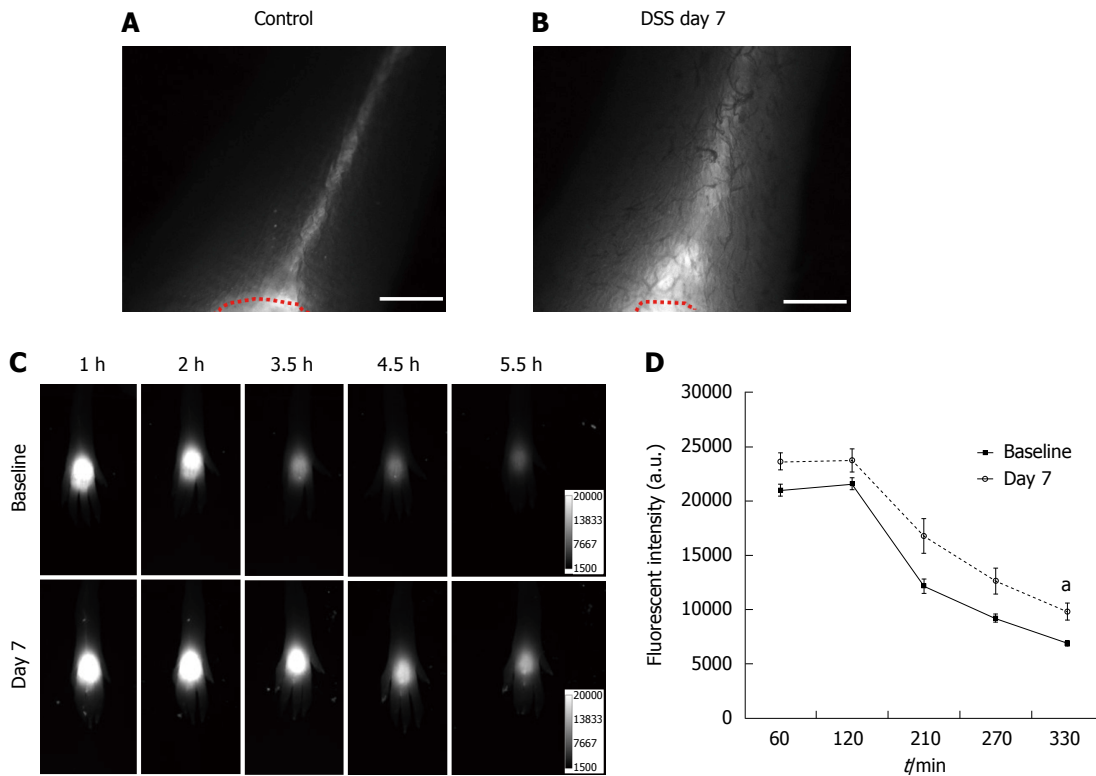


Figure 3 Near-infrared fluorescence imaging after id injection of indocyanine green in the dorsal aspect of the hind paw. NIR fluorescent images of the foot in control mice (A) and mice treated with dextran sulfate sodium (DSS) for 7 d (B) after id injection of 2 μ L of indocyanine green (ICG) in the dorsal aspect of the foot. A red dotted line delineates the ICG injection area. Representative fluorescent images in the foot of a mouse 1, 2, 3.5, 4.5, and 5.5 h after id injection of 2 μ L of Alexa680-BSA prior to (baseline), and 7 d after DSS treatment displayed the clearance of Alexa680-BSA from the depot over time (C). Quantification of the fluorescent intensities (D) remaining in the depot of Alexa680-BSA in the skin of mice treated with DSS for 7 d ($n = 7$; grey open circle) showed higher fluorescent intensity over time as compared to baseline (filled black square), which was statistically significant at 5.5 h ($P = 0.01$) in comparison to control mice. $^aP < 0.05$. Scale bar = 1 mm.

lymphangiogenesis and lymph flow^[21,22], suggesting that stimulation of functional lymphangiogenesis using VEGF-C can provide a novel therapeutic strategy for IBD. It is known that DSS causes damage to the intestinal mucosal barrier, allowing permeability of bacteria and other luminal antigens into the mucosa, thus resulting in gut inflammation^[23]. The distal colon is severely damaged with histopathological features including loss of crypts, ulceration/erosion, and edema as well as increased immune cell infiltration in the DSS model^[23]. It has also been shown that the small intestine was also damaged in response to DSS^[24,25]. Our *in situ* data after oral gavage of Bodipy-FL-C16 showed significantly fewer functional lymphatic vessels were observed in the mesentery of mice with DSS-induced acute colitis (Figure 2B), as detected by fluorescence, when compared to control (Figure 2A), due to DSS-induced disruption of intestinal and lymphatic integrity. A previous study also showed fewer functional lymphatics in TNBS-treated mice than sham animals^[5]. Bodipy-FL-C16, a fluorescently-labeled 16-carbon chain fatty acid, has been used as a lipid tracer to invasively study lymphatic architecture and function in mesenteric lymphatics^[26-29]. Previous data has demonstrated that mice with DSS-induced colitis had decreased food and water intake and body fat content as well as a disturbance of lipid

and energy metabolism as compared to control^[30,31]. Therefore, it is likely that normal fat absorption could be impaired as well. Thus, our observed impaired uptake of Bodipy-FL-C16 by mesenteric lymphatics in mice with DSS-induced colitis may also be due to metabolic alterations. A recent report showed significantly increased lymph flow in the acute phase of colitis (*i.e.*, C57BL/6 mice treated with 2.5% DSS for 7 d) as compared to control, by indirectly measuring remaining blue dye in the colon 16 h after an injection of the dye into the colonic mucosa^[32]. In our study, we did not measure the extent of lymph flow in the mesenteric lymphatic vessels. Therefore, further studies are needed to assess whether fewer mesenteric lymphatic vessels observed in our study show an increase in lymph flow during DSS-induced acute colitis. Since acute DSS-induced mucosal injury is dependent on not only DSS concentration, but also strain of mouse^[23], it is possible that the extent of acute injury due to different DSS concentrations and/or mouse strain may affect uptake of a lipid tracer.

Although the association of EIMs with IBD has been recognized, the pathologic mechanisms of EIMs are largely unknown. Adams *et al.*^[33] proposed the mechanism by which mucosal T cells are recruited to the liver in response to abnormally expressed endothelial-cell adhesion molecules and chemokines.

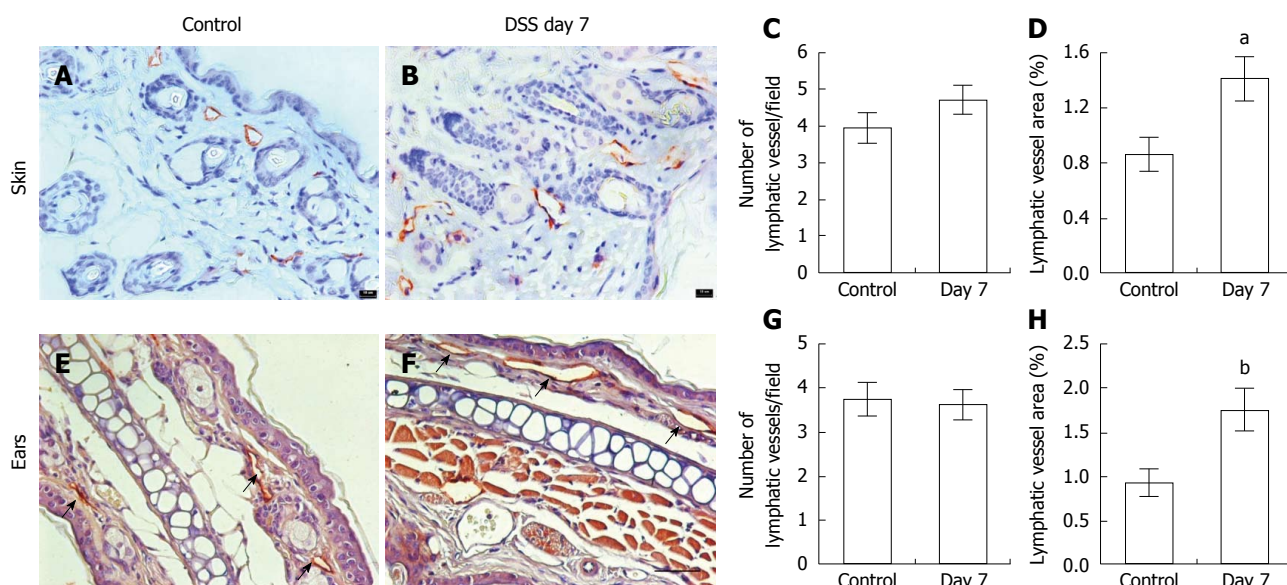


Figure 4 Immunohistochemical assessment of lymphatic vessels using antibodies to LYVE-1. In the skin (A) and ears (E, arrows) of control ($n = 5$ skin; $n = 7$ ear) and mice with dextran sulfate sodium (DSS)-induced acute colitis (B, F; $n = 6$ skin; $n = 9$ ears). Computer-assisted image analysis showed no difference in the number of lymphatic vessels per field (C, G) but increased lymphatic vessel area in both skin and ears (D, H) compared to control mice. Data presented as mean \pm SE. ^a $P < 0.05$, ^b $P < 0.01$ vs control. Scale bar = 100 μ m (C, D).

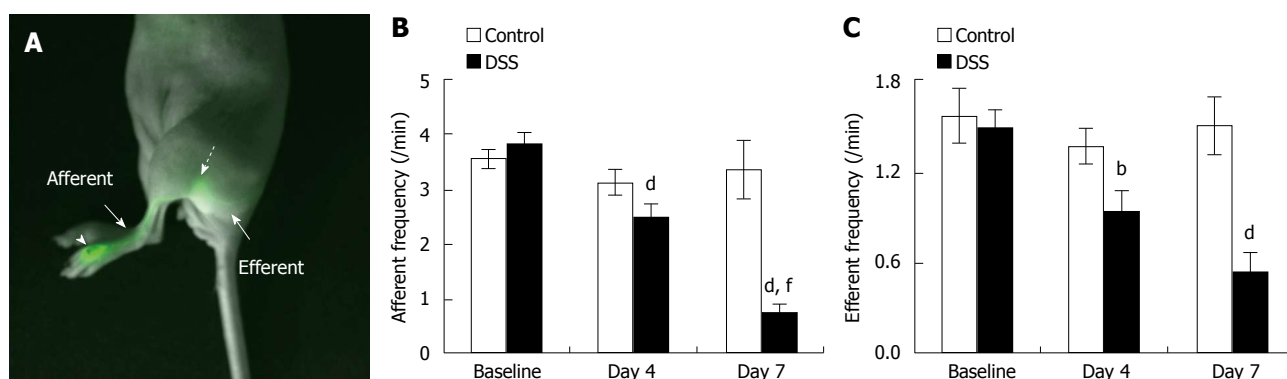


Figure 5 Lymphatic contractile function in the skin of mice with dextran sulfate sodium-induced acute colitis. Overlay of fluorescent and white light images showing lymphatic drainage of indocyanine green (ICG) from the foot, where ICG was injected (arrowhead), to the popliteal LN (broken arrow) via the popliteal afferent lymphatic vessel (A). The quantification of lymphatic contractility in the popliteal afferent (B) and efferent (C) lymphatic vessels in the foot of mice prior to 4, and 7 d after DSS alone ($n = 21$). Data represent mean \pm SE. ^b $P < 0.01$, ^d $P < 0.001$ vs baseline; ^f $P < 0.001$ vs day 4.

Therefore, T cells are exposed to hepatic antigens, and thus liver damage occurs. Aberrant homing of mucosal T cells and excessive secretion of inflammatory cytokines have also been suggested to be responsible for skin and other EIMs of IBD^[33]. Inflammatory cytokines, including TNF- α , have an important role in the recruitment of immune cells to the sites of tissue damage^[34]. TNF- α has been shown to play an important role in the pathogenesis of IBD^[34]. Thus, anti-TNF- α antibodies, such as infliximab, are used to treat IBD as well as skin EIMs, such as erythema nodosum. However, recent studies showed that anti-TNF antibodies, which are also used for the treatment of psoriasis, can cause psoriasiform skin lesions in patients with IBD^[35]. It has been demonstrated that IL-17A/IL-22-secreting Th17 cells and interferon (IFN)- γ -secreting Th1 cells are responsible for these lesions

and anti-IL-12/IL-23 antibody treatment is an effective therapy for anti-TNF antibody-induced psoriasis^[35]. IL-23 is known to be one of the major players in the pathogenesis of IBD^[34]. IL-23 is highly expressed in pyoderma gangrenosum and treatment with a monoclonal antibody ustekinumab (IL-12/23 IgG1) resulted in clinical resolution of the lesions^[36].

Studies have shown that DSS-treatment results in extra-intestinal inflammation^[37], thus stimulating inflammation by inducing the secretion of cytokines and inflammatory mediators that are transported to the lymphatic and/or blood circulation^[38]. Elevated levels of IL-6, IL-17, TNF- α , and keratinocyte-derived chemokine (KC) have been observed in mice with acute DSS-colitis; however, in chronic DSS colitis after 4 cycles of DSS (3%) for 7 d/cycle and 10 d of normal drinking water in between each cycle, significantly

elevated levels of IL-6, IFN- γ , IL-4, and IL-10 were observed as compared to control mice^[38]. We found significantly increased levels of both IL-6 (control vs DSS, 12.37 ± 8.73 vs 34.77 ± 9.25 in arbitrary unit, $P = 0.035$) and TNF- α (control vs DSS, 0.87 ± 0.61 vs 24.92 ± 5.71 , $P = 0.006$) in skin of DSS-treated mice compared to control mice. We have previously shown that locally administered pro-inflammatory cytokines such as TNF- α , IL-1 β , and IL-6 inhibit systemic lymphatic function^[39].

Preclinical and clinical studies showed that NO may be involved in GI inflammation and play a pathologic role in IBD^[40]. NO has been implicated as a mediator of tissue injury in the DSS-induced colitis model^[40,41]. Significantly increased NO production from inducible NO synthase (iNOS) was observed in the circulation and other systemic organs in mice with DSS-induced acute inflammation^[40-43]. We observed a significant increase in serum NO_x levels in mice (19 ± 1.9 $\mu\text{mol/L}$) with DSS-induced colitis as compared to control mice (12.8 ± 1.2 $\mu\text{mol/L}$, $P < 0.05$). However, it has also been reported that serum NO_x concentration was significantly increased in iNOS knockout (iNOS^{-/-}) mice over a 7 d DSS exposure as compared to untreated iNOS^{-/-} mice, suggesting that other NOS isoforms can also generate NO_x^[44]. NO has an inhibitory effect on lymphatic pump function under physiological or pathological conditions^[29,45,46], although lymphatic responses to NOS inhibition using pharmacological agents differ depending on experimental conditions^[47-51]. Liao *et al.*^[46] showed that under normal conditions endothelial NOS (eNOS) produces NO in lymphatic endothelial cells that maintains lymphatic contractions; however, at the peak of oxazolone-induced skin inflammation on day 4, increased NO production by iNOS expressing CD11b⁺Gr1⁺ cells overwhelms the eNOS-produced NO to inhibit lymphatic contractility. They also found that iNOS^{-/-} mice with oxazolone-induced skin inflammation did not change lymphatic contractility at 4 d after inflammation^[46]. Therefore, NO, together with pro-inflammatory cytokines, may affect dermal lymphatic vessel function in DSS-induced acute colitis.

Previous studies demonstrated that Balb/c mice treated with DSS for 5-7 d developed acute colitis as observed in our studies; however, Balb/c mice completely recovered 4 weeks after DSS removal as evidenced by histopathology and cytokine levels^[52]. Our preliminary data in mice treated with 2% DSS for 7 d, followed by 7 d of water, showed significantly decreased lymphatic contractility 7 d after DSS treatment as compared to baseline (Baseline vs Day 7, 4.2 ± 1.5 vs 1.6 ± 0.4 , $P < 0.001$); however, we observed recovery of lymphatic contractile function in the popliteal afferent lymphatic vessels at day 14, although it was not significantly different from that on Day 7 (Day 7 vs Day 14, 1.6 ± 0.4 vs 2.6 ± 0.5 , $P = 0.154$). Mice regained their body weight 7 d after DSS

removal (changes in body weight; baseline vs day 7 vs day 14, 100% vs 95% \pm 1.5% vs 100.4% \pm 1.3%), indicating that the process of recovery of lymphatic function from acute colitis was underway. Additional work is required to determine whether chronic gut inflammation or other chemically-induced acute models of intestinal inflammation such as TNBS-, oxazolone-mediated colitis, or genetically-modified models of colitis, lead to systemically impaired lymphatic function and/or architecture as assessed by NIRF imaging, and to investigate the effects of dissimilar cytokine/chemokine profiles that have been observed in different animal models^[38]. Indeed, a previous study demonstrated distinct cytokine profiles even between acute and chronic DSS colitis^[38]. Therefore, this information would provide additional insights in understanding the complex nature of IBD and its EIMs and how alterations to the lymphatics play a role in the pathogenesis of this disease, thus leading toward better disease management.

In conclusion, we have shown that acute inflammation induced by DSS in mice is associated with changes of dermal lymphatic architecture and function. The NIRF imaging technique employed in this study can be used to image altered lymphatic function and architecture in response to other types of systemic diseases with cutaneous involvement and likely assess lymphatic responses during therapy.

ACKNOWLEDGMENTS

The authors would like to thank Holly Robinson and Gabriel Dickinson for technical assistance with the mice used in these experiments; and Drs. Melissa B. Aldrich and Eva M. Sevick-Muraca for scientific review of this manuscript.

COMMENTS

Background

Inflammatory bowel disease (IBD) and extra-intestinal manifestations are characterized by an influx of inflammatory cells which secrete pro-inflammatory cytokines. The lymphatic system is an active and integral part of the immune system as well as a mediator of fluid return to the blood vasculature. Recent data suggests that the lymphatic system plays an important role in the pathogenesis of IBD and extra-intestinal manifestations. However, it is unknown whether gut inflammation systemically affects the lymphatics.

Research frontiers

Abnormal lymphatic function and architecture are implicated in a number of pathological conditions including edema, obesity, and immune dysfunction. Lymphatic biology has become a hot research topic and the use of near-infrared fluorescence (NIRF) imaging to investigate the role of lymphatics *in vivo* in health and disease allows the interrogation of lymphatic dysfunction in animal and man.

Innovations and breakthroughs

This is the first study investigating dermal lymphatic function and anatomy in mice with dextran sulfate sodium (DSS)-induced acute colitis. Current data demonstrates that DSS-induced colitis systemically affects the lymphatics, inducing dilation of lymphatic vessels and reducing lymphatic contractile

function in peripheral skin tissues.

Applications

The authors' observations have implications for the pathophysiology of extra-intestinal manifestations in IBD. They demonstrate that DSS-induced colitis is accompanied by impaired lymphatic function and drainage, both locally and systemically. Noninvasive functional lymphatic imaging can provide early diagnosis, risk stratification, and monitoring of lymphatic response to intervention with the appropriate therapy.

Terminology

The lymphatics consist of two major types of vessels, the initial lymphatics and the contractile, collecting lymphatics. The collecting lymphatic vessels have a unique, dynamic contractile characteristic critical to lymph flow. The collecting lymphatics have functional units, called lymphangions, which are spontaneous contractile subunits bound by "secondary valves" which prevent backflow and ensure unidirectional flow. Fluid accumulates in lymphangions before being propelled to the next sequential lymphangion, which is generated by the coordinated contractions of lymphatic vascular smooth muscle cells.

Peer-review

Authors evaluate whether dermal lymphatic function and architecture are systemically altered in DSS-induced acute colitis. The authors demonstrate that lymphatics are locally and systemically altered in acute colitis by the use of NIRF lymphatic imaging. The study is interesting and well structured.

REFERENCES

- 1 **Bouma G**, Strober W. The immunological and genetic basis of inflammatory bowel disease. *Nat Rev Immunol* 2003; **3**: 521-533 [PMID: 12876555 DOI: 10.1038/nri1132]
- 2 **Danese S**, Semeraro S, Papa A, Roberto I, Scaldaferrri F, Fedeli G, Gasbarrini G, Gasbarrini A. Extraintestinal manifestations in inflammatory bowel disease. *World J Gastroenterol* 2005; **11**: 7227-7236 [PMID: 16437620 DOI: 10.3748/wjg.v11.i46.7227]
- 3 **Huang BL**, Chandra S, Shih DQ. Skin manifestations of inflammatory bowel disease. *Front Physiol* 2012; **3**: 13 [PMID: 22347192 DOI: 10.3389/fphys.2012.00013]
- 4 **Trost LB**, McDonnell JK. Important cutaneous manifestations of inflammatory bowel disease. *Postgrad Med J* 2005; **81**: 580-585 [PMID: 16143688 DOI: 10.1136/pgmj.2004.031633]
- 5 **Wu TF**, Carati CJ, Macnaughton WK, von der Weid PY. Contractile activity of lymphatic vessels is altered in the TNBS model of guinea pig ileitis. *Am J Physiol Gastrointest Liver Physiol* 2006; **291**: G566-G574 [PMID: 16675748 DOI: 10.1152/ajpgi.00058.2006]
- 6 **Alexander JS**, Chaitanya GV, Grisham MB, Boktor M. Emerging roles of lymphatics in inflammatory bowel disease. *Ann N Y Acad Sci* 2010; **1207** Suppl 1: E75-E85 [PMID: 20961310 DOI: 10.1111/j.1749-6632.2010.05757.x]
- 7 **Heatley RV**, Bolton PM, Hughes LE, Owen EW. Mesenteric lymphatic obstruction in Crohn's disease. *Digestion* 1980; **20**: 307-313 [PMID: 7390055]
- 8 **Kovi J**, Duong HD, Hoang CT. Ultrastructure of intestinal lymphatics in Crohn's disease. *Am J Clin Pathol* 1981; **76**: 385-394 [PMID: 6117198]
- 9 **Olszewski WL**. The lymphatic system in body homeostasis: physiological conditions. *Lymphat Res Biol* 2003; **1**: 11-21; discussion 21-24 [PMID: 15624317]
- 10 **Angeli V**, Randolph GJ. Inflammation, lymphatic function, and dendritic cell migration. *Lymphat Res Biol* 2006; **4**: 217-228 [PMID: 17394405 DOI: 10.1089/lrb.2006.4406]
- 11 **Kwon S**, Sevick-Muraca EM. Noninvasive quantitative imaging of lymph function in mice. *Lymphat Res Biol* 2007; **5**: 219-231 [PMID: 18370912]
- 12 **Wirtz S**, Neufert C, Weigmann B, Neurath MF. Chemically induced mouse models of intestinal inflammation. *Nat Protoc* 2007; **2**: 541-546 [PMID: 17406617 DOI: 10.1038/nprot.2007.41]
- 13 **Goto H**, Takemura N, Ogasawara T, Sasajima N, Watanabe J, Ito H,

- Morita T, Sonoyama K. Effects of fructo-oligosaccharide on DSS-induced colitis differ in mice fed nonpurified and purified diets. *J Nutr* 2010; **140**: 2121-2127 [PMID: 20943955 DOI: 10.3945/jn.110.125948]
- 14 **Kwon S**, Sevick-Muraca EM. Functional lymphatic imaging in tumor-bearing mice. *J Immunol Methods* 2010; **360**: 167-172 [PMID: 20600076]
- 15 **Dadras SS**, Lange-Asschenfeldt B, Velasco P, Nguyen L, Vora A, Muzikansky A, Jahnke K, Hauschild A, Hirakawa S, Mihm MC, Detmar M. Tumor lymphangiogenesis predicts melanoma metastasis to sentinel lymph nodes. *Mod Pathol* 2005; **18**: 1232-1242 [PMID: 15803182]
- 16 **Kaser A**, Zeissig S, Blumberg RS. Inflammatory bowel disease. *Annu Rev Immunol* 2010; **28**: 573-621 [PMID: 20192811 DOI: 10.1146/annurev-immunol-030409-101225]
- 17 **Danese S**. Role of the vascular and lymphatic endothelium in the pathogenesis of inflammatory bowel disease: 'brothers in arms'. *Gut* 2011; **60**: 998-1008 [PMID: 21212253 DOI: 10.1136/gut.2010.207480]
- 18 **Deban L**, Correale C, Vetrano S, Malesci A, Danese S. Multiple pathogenic roles of microvasculature in inflammatory bowel disease: a Jack of all trades. *Am J Pathol* 2008; **172**: 1457-1466 [PMID: 18458096 DOI: 10.2353/ajpath.2008.070593]
- 19 **von der Weid PY**, Rehal S, Ferraz JG. Role of the lymphatic system in the pathogenesis of Crohn's disease. *Curr Opin Gastroenterol* 2011; **27**: 335-341 [PMID: 21543977 DOI: 10.1097/MOG.0b013e3283476e8f]
- 20 **Ganta VC**, Cromer W, Mills GL, Traylor J, Jennings M, Daley S, Clark B, Mathis JM, Bernas M, Boktor M, Jordan P, Witte M, Alexander JS. Angiopoietin-2 in experimental colitis. *Inflamm Bowel Dis* 2010; **16**: 1029-1039 [PMID: 19902545 DOI: 10.1002/ibd.21150]
- 21 **D'Alessio S**, Tacconi C, Fiocchi C, Danese S. Advances in therapeutic interventions targeting the vascular and lymphatic endothelium in inflammatory bowel disease. *Curr Opin Gastroenterol* 2013; **29**: 608-613 [PMID: 24100721 DOI: 10.1097/MOG.0b013e328365d37c]
- 22 **Jurisc G**, Sundberg JP, Detmar M. Blockade of VEGF receptor-3 aggravates inflammatory bowel disease and lymphatic vessel enlargement. *Inflamm Bowel Dis* 2013; **19**: 1983-1989 [PMID: 23835443 DOI: 10.1097/MIB.0b013e31829292f7]
- 23 **Perše M**, Cerar A. Dextran sodium sulphate colitis mouse model: traps and tricks. *J Biomed Biotechnol* 2012; **2012**: 718617 [PMID: 22665990 DOI: 10.1155/2012/718617]
- 24 **Takahashi S**, Kawamura T, Kanda Y, Taniguchi T, Nishizawa T, Iiai T, Hatakeyama K, Abo T. Multipotential acceptance of Peyer's patches in the intestine for both thymus-derived T cells and extrathymic T cells in mice. *Immunol Cell Biol* 2005; **83**: 504-510 [PMID: 16174100 DOI: 10.1111/j.1440-1711.2005.01361.x]
- 25 **Geier MS**, Smith CL, Butler RN, Howarth GS. Small-intestinal manifestations of dextran sulfate sodium consumption in rats and assessment of the effects of Lactobacillus fermentum BR11. *Dig Dis Sci* 2009; **54**: 1222-1228 [PMID: 19005763 DOI: 10.1007/s10620-008-0495-4]
- 26 **Kassis T**, Kohan AB, Weiler MJ, Nipper ME, Cornelius R, Tso P, Dixon JB. Dual-channel in-situ optical imaging system for quantifying lipid uptake and lymphatic pump function. *J Biomed Opt* 2012; **17**: 086005 [PMID: 23224192 DOI: 10.1117/1.JBO.17.8.086005]
- 27 **Harvey NL**, Srinivasan RS, Dillard ME, Johnson NC, Witte MH, Boyd K, Sleeman MW, Oliver G. Lymphatic vascular defects promoted by Prox1 haploinsufficiency cause adult-onset obesity. *Nat Genet* 2005; **37**: 1072-1081 [PMID: 16170315]
- 28 **Jeon BH**, Jang C, Han J, Kataru RP, Piao L, Jung K, Cha HJ, Schwendener RA, Jang KY, Kim KS, Alitalo K, Koh GY. Profound but dysfunctional lymphangiogenesis via vascular endothelial growth factor ligands from CD11b+ macrophages in advanced ovarian cancer. *Cancer Res* 2008; **68**: 1100-1109 [PMID: 18281485 DOI: 10.1158/0008-5472.CAN-07-2572]
- 29 **Ribera J**, Pauta M, Melgar-Lesmes P, Tugues S, Fernández-Varo

- G, Held KF, Soria G, Tudela R, Planas AM, Fernández-Hernando C, Arroyo V, Jiménez W, Morales-Ruiz M. Increased nitric oxide production in lymphatic endothelial cells causes impairment of lymphatic drainage in cirrhotic rats. *Gut* 2013; **62**: 138-145 [PMID: 22267600 DOI: 10.1136/gutjnl-2011-300703]
- 30 **Dong F**, Zhang L, Hao F, Tang H, Wang Y. Systemic responses of mice to dextran sulfate sodium-induced acute ulcerative colitis using 1H NMR spectroscopy. *J Proteome Res* 2013; **12**: 2958-2966 [PMID: 23651354 DOI: 10.1021/pr4002383]
- 31 **Melgar S**, Bjursell M, Gerdin AK, Svensson L, Michaëlsson E, Bohlooly-Y M. Mice with experimental colitis show an altered metabolism with decreased metabolic rate. *Am J Physiol Gastrointest Liver Physiol* 2007; **292**: G165-G172 [PMID: 16844678 DOI: 10.1152/ajpgi.00152.2006]
- 32 **D'Alessio S**, Correale C, Tacconi C, Gandelli A, Pietrogrande G, Vetrano S, Genua M, Arena V, Spinelli A, Peyrin-Biroulet L, Fiocchi C, Danese S. VEGF-C-dependent stimulation of lymphatic function ameliorates experimental inflammatory bowel disease. *J Clin Invest* 2014; **124**: 3863-3878 [PMID: 25105363 DOI: 10.1172/JCI72189]
- 33 **Adams DH**, Eksteen B. Aberrant homing of mucosal T cells and extra-intestinal manifestations of inflammatory bowel disease. *Nat Rev Immunol* 2006; **6**: 244-251 [PMID: 16498453 DOI: 10.1038/nri1784]
- 34 **Strober W**, Fuss IJ. Proinflammatory cytokines in the pathogenesis of inflammatory bowel diseases. *Gastroenterology* 2011; **140**: 1756-1767 [PMID: 21530742 DOI: 10.1053/j.gastro.2011.02.016]
- 35 **Tillack C**, Ehmann LM, Friedrich M, Laubender RP, Papay P, Vogelsang H, Stallhofer J, Beigel F, Bedynek A, Wetzke M, Maier H, Koburger M, Wagner J, Glas J, Diegelmann J, Koglin S, Dombrowski Y, Schaubert J, Wollenberg A, Brand S. Anti-TNF antibody-induced psoriasiform skin lesions in patients with inflammatory bowel disease are characterised by interferon- γ -expressing Th1 cells and IL-17A/IL-22-expressing Th17 cells and respond to anti-IL-12/IL-23 antibody treatment. *Gut* 2014; **63**: 567-577 [PMID: 23468464 DOI: 10.1136/gutjnl-2012-302853]
- 36 **Guenova E**, Teske A, Fehrenbacher B, Hoerber S, Adamczyk A, Schaller M, Hoetzenecker W, Biedermann T. Interleukin 23 expression in pyoderma gangrenosum and targeted therapy with ustekinumab. *Arch Dermatol* 2011; **147**: 1203-1205 [PMID: 21680759 DOI: 10.1001/archdermatol.2011.168]
- 37 **Kitajima S**, Takuma S, Morimoto M. Tissue distribution of dextran sulfate sodium (DSS) in the acute phase of murine DSS-induced colitis. *J Vet Med Sci* 1999; **61**: 67-70 [PMID: 10027168]
- 38 **Alex P**, Zachos NC, Nguyen T, Gonzales L, Chen TE, Conklin LS, Centola M, Li X. Distinct cytokine patterns identified from multiplex profiles of murine DSS and TNBS-induced colitis. *Inflamm Bowel Dis* 2009; **15**: 341-352 [PMID: 18942757 DOI: 10.1002/ibd.20753]
- 39 **Aldrich MB**, Sevick-Muraca EM. Cytokines are systemic effectors of lymphatic function in acute inflammation. *Cytokine* 2013; **64**: 362-369 [PMID: 23764549 DOI: 10.1016/j.cyto.2013.05.015]
- 40 **Kolios G**, Valatas V, Ward SG. Nitric oxide in inflammatory bowel disease: a universal messenger in an unsolved puzzle. *Immunology* 2004; **113**: 427-437 [PMID: 15554920 DOI: 10.1111/j.1365-2567.2004.01984.x]
- 41 **Cross RK**, Wilson KT. Nitric oxide in inflammatory bowel disease. *Inflamm Bowel Dis* 2003; **9**: 179-189 [PMID: 12792224]
- 42 **Saijo F**, Milsom AB, Bryan NS, Bauer SM, Vowinkel T, Ivanovic M, Andry C, Granger DN, Rodriguez J, Feelisch M. On the dynamics of nitrite, nitrate and other biomarkers of nitric oxide production in inflammatory bowel disease. *Nitric Oxide* 2010; **22**: 155-167 [PMID: 20005300 DOI: 10.1016/j.niox.2009.11.009]
- 43 **Kubes P**. Inducible nitric oxide synthase: a little bit of good in all of us. *Gut* 2000; **47**: 6-9 [PMID: 10861252]
- 44 **Beck PL**, Xavier R, Wong J, Ezedi I, Mashimo H, Mizoguchi A, Mizoguchi E, Bhan AK, Podolsky DK. Paradoxical roles of different nitric oxide synthase isoforms in colonic injury. *Am J Physiol Gastrointest Liver Physiol* 2004; **286**: G137-G147 [PMID: 14665440 DOI: 10.1152/ajpgi.00309.2003]
- 45 **Shirasawa Y**, Ikomi F, Ohhashi T. Physiological roles of endogenous nitric oxide in lymphatic pump activity of rat mesentery in vivo. *Am J Physiol Gastrointest Liver Physiol* 2000; **278**: G551-G556 [PMID: 10762608]
- 46 **Liao S**, Cheng G, Conner DA, Huang Y, Kucherlapati RS, Munn LL, Ruddle NH, Jain RK, Fukumura D, Padera TP. Impaired lymphatic contraction associated with immunosuppression. *Proc Natl Acad Sci USA* 2011; **108**: 18784-18789 [PMID: 22065738 DOI: 10.1073/pnas.1116152108]
- 47 **Gasheva OY**, Zawieja DC, Gashev AA. Contraction-initiated NO-dependent lymphatic relaxation: a self-regulatory mechanism in rat thoracic duct. *J Physiol* 2006; **575**: 821-832 [PMID: 16809357]
- 48 **Koller A**, Mizuno R, Kaley G. Flow reduces the amplitude and increases the frequency of lymphatic vasomotion: role of endothelial prostanooids. *Am J Physiol* 1999; **277**: R1683-R1689 [PMID: 10600914]
- 49 **Mizuno R**, Dörnyei G, Koller A, Kaley G. Myogenic responses of isolated lymphatics: modulation by endothelium. *Microcirculation* 1997; **4**: 413-420 [PMID: 9431509]
- 50 **Mizuno R**, Koller A, Kaley G. Regulation of the vasomotor activity of lymph microvessels by nitric oxide and prostaglandins. *Am J Physiol* 1998; **274**: R790-R796 [PMID: 9530247]
- 51 **Bohlen HG**, Wang W, Gashev A, Gasheva O, Zawieja D. Phasic contractions of rat mesenteric lymphatics increase basal and phasic nitric oxide generation in vivo. *Am J Physiol Heart Circ Physiol* 2009; **297**: H1319-H1328 [PMID: 19666850 DOI: 10.1152/ajpheart.00039.2009]
- 52 **Melgar S**, Karlsson A, Michaëlsson E. Acute colitis induced by dextran sulfate sodium progresses to chronicity in C57BL/6 but not in BALB/c mice: correlation between symptoms and inflammation. *Am J Physiol Gastrointest Liver Physiol* 2005; **288**: G1328-G1338 [PMID: 15637179 DOI: 10.1152/ajpgi.00467.2004]

P- Reviewer: De Minicis S, Hayashi S **S- Editor:** Yu J
L- Editor: A **E- Editor:** Wang CH





Published by **Baishideng Publishing Group Inc**

8226 Regency Drive, Pleasanton, CA 94588, USA

Telephone: +1-925-223-8242

Fax: +1-925-223-8243

E-mail: bpgoffice@wjgnet.com

Help Desk: <http://www.wjgnet.com/esps/helpdesk.aspx>

<http://www.wjgnet.com>



ISSN 1007-9327

